Helmholtz-Zentrum Dresden-Rossendorf (HZDR)

HELMHOLTZ ZENTRUM
DRESDEN ROSSENDORF

Magnetocaloric Effect with Very Small Magnetic Hysteresis Losses of CoMn1-xTixGe Alloys

Yildirim, O.; Tozkoparan, O.; Yuzuak, E.; Elerman, Y.; Dincer, I.;

Originally published:

August 2017

Metallurgical and Materials Transactions A 48(2017)11, 5733-5737

DOI: https://doi.org/10.1007/s11661-017-4282-8

Perma-Link to Publication Repository of HZDR:

https://www.hzdr.de/publications/Publ-24003

Release of the secondary publication
on the basis of the German Copyright Law § 38 Section 4.

Giant magnetocaloric effect with very small magnetic hysteresis losses of $CoMn_{1-x}Ti_xGe$ alloys

OGUZ YILDIRIM[1], ONUR TOZKOPARAN[2], ERCUMENT YUZUAK[3], YALCIN ELERMAN[2], ILKER DINCER*[,2]

[1]Institute of Ion Beam Physics and Materials Research, Helmholtz-Zentrum Dresden-Rossendorf, 01314 Dresden, Germany, o.yildirim@hzdr.de (O. Yildirim)
[2]Department of Engineering Physics, Faculty of Engineering, Ankara University, 06100 Besevler, Ankara Turkey, onur_tozkoparan@hotmail.com (O. Tozkoparan), elerman@ankara.edu.tr (Y. Elerman), idincer@eng.ankara.edu.tr (I. Dincer)
[3]Department of Nanotechnology Engineering, Faculty of Engineering, Recep Tayyip Erdogan University, 53100 Rize, Turkey, ercumentyuzuak@yahoo.com (E. Yuzuak)
*Corresponding author: idincer@eng.ankara.edu.tr

Abstract- The effects of Ti substitution for Mn and heat treatment on structural, magnetic and magnetocaloric properties of CoMnGe alloy have been investigated by electron microscopy, X-ray diffraction, calorimetric and magnetic measurements. According to X-ray diffraction measurements, the $CoMn_{1-x}Ti_xGe$ alloys are in a single phase, hexagonal structure at room temperature. It is found that the as-cast $CoMn_{0.95}Ti_{0.05}Ge$ alloy shows a magnetostructural phase transition close to room temperature. The transition shows a large magnetic entropy change and a small hysteresis in the isothermal magnetic field dependent magnetization measurements. Upon annealing, the transition temperature decreases slightly. The decrease in temperature is accompanied by a significant increase in the magnetic entropy change, i.e., magnetic entropy change at 1 T field change was increased from -3.3 $J.kg^{-1}.K^{-1}$ to -6.3 $J.kg^{-1}.K^{-1}$. Moreover, after annealing, hysteresis losses reduced significantly for ΔH=7 T. Accordingly, we report that the heat treatment has a significant effect on magnetocaloric properties of the $CoMn_{0.95}Ti_{0.05}Ge$ alloy.

1. Introduction

During past two decades, an increasing attention has been paid to magnetic refrigeration technology based on magnetocaloric effect (MCE), because this technology is considered a possible alternative to the widely used conventional gas compression refrigeration. The principle advantages of magnetic refrigeration compared with conventional refrigeration are: (i) improved refrigerator efficiency, (ii) reduced CO_2 production from the energy savings, and (iii) solid, non-volatile refrigerant, eliminating greenhouse gas refrigerants [1–5].

The materials which exhibit a giant MCE offer scope for magnetic refrigeration technology around room temperature. Recently, Co-Mn-Ge based alloys have been proposed as magnetocaloric materials owing to their remarkable first-order phase transition feature. CoMnGe alloy shows a diffusionless martensitic structural transition from a Ni_2In-type hexagonal structure (space group $P6_3/mmc$) to a TiNiSi-type orthorhombic structure (space group Pnma) around 650 K (376.85 °C) and a magnetic transition from paramagnetism to ferromagnetism at T_C= 345 K (71.85 °C) [7, 8]. The structural and magnetic phase transition temperatures of CoMnGe alloy are sensitive to the compositional modifications, i.e., substitution, doping or interstitials. Those modifications on CoMnGe alloy can simultaneously change the structural and magnetic transition temperatures and offers the possibility to overlap them at the same temperature. Thus, the magnetostructural phase transition can be observed around room temperature on Co-Mn-Ge based alloys with substitution, doping or interstitials.

By interstitially adding some boron atoms to CoMnGe, the structural and the magnetic transition can be controlled to coincide. As a result, $CoMnGeB_x$ and $CoMnGe_{1-x}Ga_xB_{0.015}$ alloys showed giant MCE around room temperature [9, 10]. In addition to interstitials, the giant MCE can also

be attained by substituting some Cr or V for Mn atoms in MnCoGe [11, 12]. Similarly, due to comparable atomic radii and electronic structures, Ti is a promising candidate to replace Mn within the CoMnGe system. Substituting Mn with Ti is expected to change electron per atom ratio, which in turn may change magnetic properties of the system and lead to a large MCE. The structural, magnetic and magnetocaloric properties of $CoMn_{1-x}Ti_xGe$ alloys have been investigated by electron microscopy, X-ray diffraction, calorimetric and magnetic measurements and the MCE has been derived from the M(H) curves.

2. Experimental

The polycrystalline samples of $CoMn_{1-x}Ti_xGe$ (x=0.05 and 0.10) alloys were prepared by conventional arc melting the appropriate amounts of high purity elements (Co 99.9%, Mn 99.9%, Ge 99.9999%, Ti 99.999%). The polycrystalline samples were melted several times on water cooled Cu crucible under Argon atmosphere to ensure the homogeneity. The samples were sealed in a quartz ampoule and annealed at 1123 K (849.85 °C) for 5 days and then quenched in ice water. Annealing conditions were chosen to achieve homogeneity over whole sample volume [11]. Compositions and homogeneity of samples were investigated by using a scanning electron microscope (SEM) equipped with x-ray energy dispersive spectroscopy (EDS) system. The X-ray diffraction (XRD) measurements using Cu Kα radiation were performed to identify crystal structure. Thermal properties of samples were characterized by using TA Instruments Q100 differential scanning calorimeter, with an empty aluminium pan as a reference. The DSC measurements were carried out in heating and cooling cycles with a scanning rate 10 K/min. The magnetization measurements were carried out using a Quantum Design 7 T physical property measurement system (PPMS). Temperature dependent magnetization measurements-M(T) were carried out field cooling (FC) and field heating (FH) directions with applied field of 150 Oe. The magnetic field dependent magnetization M(H) curves obtained 0-7 T magnetic field range and 3 K (3 °C) temperature change around phase transition temperatures.

3. Results and Discussions

Before investigating the physical properties, the EDX analysis were performed for as-cast and annealed $CoMn_{0.95}Ti_{0.05}Ge$ alloys (x=0.05 and 0.10) by using SEM, because the structural and magnetic properties depend very strongly on the composition of CoMnGe based alloys. The back-scattered electron detector analysis showed that there are no different structural phases available for these alloys after homogenization heat treatment. This means that these alloys have the uniform composition. The average compositions obtained from EDX analysis are revealed to be the nominal formula $Co_{1.01(4)}Mn_{0.93(2)}Ti_{0.05(1)}Ge_{1.01(4)}$ and $Co_{1.02(4)}Mn_{0.88(3)}Ti_{0.10(1)}Ge_{1.00(4)}$ and are within the permitted margin of error.

The room temperature X-ray diffraction patters and Rietveld refinement result of annealed $CoMn_{0.95}Ti_{0.05}Ge$ and $CoMn_{0.90}Ti_{0.10}Ge$ alloys are shown in Fig. 1. The room temperature XRD patterns were analysed using FullProf program to determine their crystal structure. The Ni_2In-type hexagonal structure (space group $P6_3/mmc$) with different unit cell parameters was observed for these alloys at room temperature. The hexagonal unit cell parameters increase with increasing Ti content (a=b=4.07(3) Å 4.08(3) Å and c=5.32(4) Å 5.34(4) Å for x=0.05 and 0.10). This is attributed to atomic radius of Mn,

which is smaller than that of Ti.

The DSC heat flow curves of as-cast and annealed $CoMn_{0.95}Ti_{0.05}Ge$ and $CoMn_{0.90}Ti_{0.10}Ge$ alloys are displayed in Fig.2. Well defined exothermic and endothermic peaks with large thermal hysteresis indicate the first-order structural phase transition for as-cast and annealed $CoMn_{0.95}Ti_{0.05}Ge$ alloy upon cooling and heating processes, respectively. The width of the thermal hysteresis of the first-order structural phase transition is 16 K (16 °C) for annealed $CoMn_{0.95}Ti_{0.05}Ge$ alloy. The small peaks with no thermal hysteresis of as-cast and annealed $CoMn_{0.90}Ti_{0.10}Ge$ alloy are related to the second-order magnetic phase transitions at Curie temperature (T_C=236 K (-37.15 °C)) of the hexagonal phase. The average integrated entropy changes from DSC curve for annealed $CoMn_{0.95}Ti_{0.05}Ge$ alloy upon warming is ΔS_{DSC}=38.9 $J.kg^{-1}.K^{-1}$.

The temperature dependence of magnetization measurements was performed for as cast and annealed $CoMn_{1-x}Ti_xGe$ (x=0.05 and 0.10) alloys to determine the influence of the heat treatment on their magnetic and magnetocaloric properties. Fig. 3 shows the temperature dependence of magnetization M(T) of $CoMn_{1-x}Ti_xGe$ (x=0.05 and 0.10) alloys in a field of 150 Oe for FC and FH modes. According to Fig. 3(a), the as-cast and annealed $CoMn_{0.95}Ti_{0.05}Ge$ alloys have a ferromagnetic order below Curie temperature and above this temperature they become paramagnetic. Moreover, in the vicinity of Curie temperature, an thermal hysteresis between FC and FH curves is observed for them. Considering the DSC results, this thermal hysteresis is attributed to a first order structural transformation. The phase transition occurs in the narrow temperature range for annealed $CoMn_{0.95}Ti_{0.05}Ge$ alloy as compared to the as-cast $CoMn_{0.95}Ti_{0.05}Ge$ alloy. The as-cast and annealed $CoMn_{0.90}Ti_{0.10}Ge$ have ferromagnetic character below T_C=236 K (-37.15 °C) and paramagnetic above this temperature. There is no thermal hysteresis between FC and FH curves (as seen in Fig. 3(b)). This means that as-cast and annealed $CoMn_{0.90}Ti_{0.10}Ge$ have no structural transition and DSC measurement confirms this result.

The magnetic field dependence of magnetization curves-M(H) for as-cast and annealed $CoMn_{0.95}Ti_{0.05}Ge$ alloys were performed for increasing and decreasing magnetic field directions in order to investigate magnetic hysteresis losses within the reverse transformation range. Fig. 4 (a) and (b) show the M(H) curves are measured for as-cast and annealed $CoMn_{0.95}Ti_{0.05}Ge$ alloys, respectively. For the as-cast sample clear magnetic hysteresis was observed in M(H) curves between 2T and 7T. However, annealed sample did not show any hysteretic behaviour in M(H) curves, indicating that field-induced phase transition could be achieved higher magnetic fields than 7T. Therefore, this also explains the absence of hysteresis losses in the annealed sample. Similarly, in $Co_{0.92}Mn_{1.07}Ge$ alloy [13], the field induced structural phase transition was observed around martensitic transition temperature-M_s in magnetic fields of B_t=7.5 T. However, the field-induced phase transition could be reached at a magnetic field about 4 T for $CoMnGe_{0.95}Ga_{0.05}$ alloy [14].

Magnetocaloric materials with no magnetic hysteresis at high magnetic fields offer a better trade-off for magnetic refrigeration technology. Thus, these alloys are of great interest for potential applications. The magnitude of MCE of a magnetocaloric material can be characterized by the isothermal magnetic entropy change (ΔS_M) in a changing magnetic field. The ΔS_M values are estimated from the M (H) curves using the Maxwell relation:

$$\Delta S_M = \int_{H_1}^{H_2} \left(\frac{\partial M}{\partial T}\right)_H dH \quad (1)$$

and its numerical expression:

$$\Delta S_M = \frac{1}{2\delta T}(\delta M_1 \delta H_1 + \delta M_n \delta H_n + 2\sum_{k=2}^{n-1} \delta M_k \delta H_k) \quad (2)$$

Here, $\delta T = T_k - T_{k-1}$ is the temperature interval between two isotherms, where n is the number of points that are measured for the two isotherms with the magnetic field changing by δH and δM is the difference in the magnetization from 1 to n and $T=(T_k+T_{k+1})/2$. Using the M(H) curves and equation (2), the isothermal entropy change ΔS_M values are determined and the ΔS_M(T, H) curves shown in Fig. 5 (a) and (b) for as-cast and annealed $CoMn_{0.95}Ti_{0.05}Ge$ alloys. As expected, the ΔS_M(T, H) values are negative (conventional MCE). While the maximum entropy change value is -22.2 $J.kg^{-1}.K^{-1}$ for as-cast $CoMn_{0.95}Ti_{0.05}Ge$ alloy, it is -40.5 $J.kg^{-1}.K^{-1}$ for annealed $CoMn_{0.95}Ti_{0.05}Ge$ alloy under the magnetic field change of 7 T. There is second maximum in the ΔS_M (T, H) curve for as-cast $CoMn_{0.95}Ti_{0.05}Ge$ alloy around 280 K (6.85 °C). This second maximum show that the magnetic phase transition (from paramagnetic to ferromagnetic with decreasing temperature) and first order structural phase transition (from hexagonal to orthorhombic) occurs at different temperatures. According to the M(T) and ΔS_M(T, H) curves, the annealing process is very important for these alloys and needed to observe the structural phase transition at the same temperature.

The experimental results of annealed $CoMn_{0.95}Ti_{0.05}Ge$ alloy and its comparison with the other similar systems are summarized in Table 1. Present and previous studies on CoMnGe based alloys show that the giant MCE is associated with the magnetostructural phase transition. The ΔS_M value (for ΔH=0-5 T) of annealed $CoMn_{0.95}Ti_{0.05}Ge$ alloy compare well with other giant MCE materials. For the materials showed magnetostructural phase transition, the giant MCE is always accompanied by an magnetic hysteresis, which reduces the cooling effciency of magnetic refrigerator. Therefore, the magnetocaloric materials with very small magnetic hysteresis, are greatly desired for the magnetic refrigeration. In table I, the comparison of the hysteresis losses is made with Gd metal which is the prototype magnetic refrigerant. A “o” indicates that the factor is essentially the same as for Gd. A “-” indicates that the property is inferior to that of Gd, and two or three minus signs indicate the hysteresis losses are much worse, or much worse than for Gd. Compared to $(NiMnSi)_{0.56}(FeNiGe)_{0.44}$ [19] $(NiMnSi)_{0.65}(Fe_2Ge)_{0.35}$ [20] systems which enables very large transition temperature window together with large entropy changes and accompanied large hysteresis losses, annealed $CoMn_{0.95}Ti_{0.05}Ge$ alloy shows comparable entropy change with no hysteresis losses. Concerning the efficient magnetic refrigeration applications, the annealed $CoMn_{0.95}Ti_{0.05}Ge$ alloy is a promising candidate with no hysteresis losses, large entropy change and low cost and nontoxic constituent elements.

In the light of our and previous results, we present the structural and magnetic phase diagram in Fig. 6 that exhibits a clear picture of the magnetostructural coupling in $CoMn_{1-x}Ti_xGe$ alloys. The structural phase transition temperature decreases with Ti content from 650 K (376.85 °C) CoMnGe alloy to 235 K (-38.15 °C) for $CoMn_{0.94}Ti_{0.06}Ge$ alloy. The Curie temperatures of the $CoMn_{1-x}Ti_xGe$ alloys decreases slightly from 345 (71.85 °C) to 236 K (-37.15 °C). The structural and magnetic phase transitions occur at the same temperature for x=0.05, i.e. this alloy shows a transition from paramagnetic hexagonal to ferromagnetic orthorhombic structure with decreasing temperature.

4. Conclusion

In conclusion, we prepared a series of $CoMn_{1-x}Ti_xGe$ alloys (x=0.05 and 0.10) alloys and investigated their structural, magnetic and magnetocaloric properties. In the $CoMn_{0.95}Ti_{0.05}Ge$ alloy, a magnetostructural phase transition with giant MCE is obtained, whereas the $CoMn_{0.90}Ti_{0.10}Ge$ alloy shows second order phase transition. The annealed $CoMn_{0.95}Ti_{0.05}Ge$ alloy gives rise to a large entropy change of -30.2 $J.kg^{-1}.K^{-1}$ for Δ=5 T. Interestingly almost zero magnetic hysteresis losses are observed in the $CoMn_{0.95}Ti_{0.05}Ge$ alloy which is of great importance from the application point of view.

Acknowledgements

This work was supported by TUBITAK (Project Number: 109T743). We thank Anja Diekmann (from department of Physikalische Chemie II, Universitaet Bielefeld) for the DSC measurements.

References

[1] A. Kitanovski, and P. W. Egolf: *J. Magn. Magn. Mater.*, 2009, vol. 321, pp. 777.

[2] V. Franco, J. S. Blázquez, B. Ingale, and A. Conde: *Annu. Rev. Mater. Res.*, 2012, vol. 42, pp. 305.

[3] J. Liu, T. Gottschall, K. P. Skokov, J. D. Moore, and O. Gutfleisch: *Nat. Mater.*, 2012, vol. 11, pp. 620.

[4] K. G. Sandeman: *Scripta. Mat.*, 2012, vol. 67, pp. 566.

[5] S. Fähler, U. K. Röβler, O. Kastner, J. Eckert, G. Eggeler, H. Emmerich, P. Entel, S. Müller, E. Quandt, and K. Albe: *Adv. Eng. Mater.*, 2012, vol. 14, pp. 10.

[6] T. Samanta, I. Dubenko, A. Quetz, J. Prestigiacomo, P. W. Adams, S. Stadler, and N. Ali: *Appl. Phys. Let.*,2013, vol. 103, pp. 042408.

[7] V. Johnson: I*norg. Chem.*, 1975, vol. 14 1975, pp. 1117.

[8] S. Niziol, A. Weselucha, W. Bazela, and A. Szytula: *Solid State Commun.*, 1981, vol. 39, pp. 1081.

[9] N. T. Trung, L. Zhang, L. Caron, K. H. J. Buschow, and E. Brück: *Appl. Phys. Lett.*, 2010, vol. 96, pp. 172504.

[10] E. Yüzüak, G. Durak, I. Dincer, and Y. Elerman: *J. Magn. Magn. Mater.*, 2014, vol. 354, pp. 195.

[11] N. T. Trung, V. Biharie, L. Zhang, L. Caron, K. H. J. Buschow, and E. Brück: *Appl. Phys. Lett.*, 2010, vol. 96, pp. 162507.

[12] S. C. Ma, Y. X. Zheng, H. C. Xuan, L. J. Shen, Q. Q. Cao, D. H. Wang, Z. C. Zhong, and Y.W. Du: *J. Magn. Magn.Mater.*, 2012, vol. 324, pp. 135.

[13] K. Koyama, M. Sakai, T. Kanomata, and K. Watanabe: *Japanese J. App. Phys.*, 2004, pp. 43, pp. 8036.

[14] I. Dincer, G. Durak, E. Yüzüak, Y. Elerman, A. M. T. Bell, and H. Ehrenberg: *J. Alloys. Comp.*, 2012, vol. 540, pp. 236.

[15] S. Yu. Dan'kov, A. M. Tishin, V. K. Pecharsky, and K. A. Gschneidner Jr.: *Phys. Rev. B*, 1998, vol. 57, pp. 3478.

[16] E. Yüzüak, I. Dincer, Y. Elerman, I. Dumkow, B. Heger, and S. Y. Emre: *J. Alloys. Comp.*, 2015, vol. 641, pp. 69.

[17] G. J. Li, E. K. Liu, H. G. Zhang, Y. J. Zhang, J. L. Chen, W. H. Wang, H. W. Zhang, G. H. Wu, and S. Y. Yu: *J.Magn. Magn. Mater.*, 2013, vol. 332, pp. 146.

[18] E. K. Liu, W. Zhu, L. Feng, J. L. Chen, W. H. Wang, G. H.Wu, H.Y. Liu, F.B. Meng, H.Z. Luo,

and Y.X. Li: *Europhys. Let.*, 2010, vol. 91, pp. 17003.

[19] C. L. Zhang, D. H. Wang, Z. D. Han, B. Qian, H. F. Shi, C. Zhu, J. Chen, and T. Z. Wang: *Appl. Phys. Let.*, 2013, vol.103, pp. 132411.

[20] C. L. Zhang, H. F. Shi, E. J. Ye, Y. G. Nie, Z. D. Han, B. Qian, and D.H. Wang: *Appl. Phys. Lett.*, 2015, vol. 107, pp. 212403.

[21] P. Shamba, J. L. Wang, J. C. Debnath, S. J. Kennedy, R. Zeng, M. F. Md. Din, F. Hong, Z. X. Cheng, A. J. Studer, and S. X. Dou: *J. Phys.: Condens. Matter*, 2013, vol. 25, pp. 056001.

[22] A. Rostamnejadi, M. Venkatesan, P. Kameli, H. Salamati and J. M. D Coey, *J. Magn. Magn. Mater.* 2011vol. 323 pp.2214.

[23] X. Zhou, W. Li, H. P. Kunkel, G. Williams and S. Zhang, *J. Appl. Phys.* 2005 vol. 97 pp.10M515

[24] J. Lyubina, J. *Appl. Phys.* 2011 vol.109 pp. 07A902

Tables

Table 1. The Curie temperature T_C (for heating mode), hysteresis losses (HL) for different magnetic field change and observed maximum ΔS_M (ΔH=0-5T) values for giant magnetocaloric materials including annealed $CoMn_{0.95}Ti_{0.05}Ge$ alloy (*This value is for ΔH=0-1T).

Material	Curie Temperature T_C (K)	Hysteresis Loses HL	Magnetic Entropy Change Value $-\Delta S_M$ ($J.kg^{-1}.K^{-1}$)	Ref.
Gd	294	$(o)^{7T}$	11.0	[15]
$CoMn_{0.95}Ti_{0.05}Ge$	277	$(o)^{7T}$	30.2	This work
$CoMnGe_{0.95}Ga_{0.05}$	317	$(---)^{7T}$	27.1	[14]
$CoMn_{0.9}Fe_{0.1}Ge$	300	$(--)^{7T}$	35.5	[16]
$Co_{0.94}Fe_{0.06}MnGe$	335	$(---)^{5T}$	27.5	[17]
$CoMnGe_{0.95}Ga_{0.05}B_{0.015}$	286	$(--)^{7T}$	20.5	[10]
$CoMn_{0.965}Ge$	307	$(----)^{13T}$	26.0	[18]
$(NiMnSi)_{0.56}(FeNiGe)_{0.44}$	292	$(-----)^{5T}$	11.5^{*}	[19]
$(NiMnSi)_{0.65}(Fe_2Ge)_{0.35}$	260	$(---)^{5T}$	38.0	[20]
$La_{0.67}Sr_{0.33}MnO_3$	375	unknown	5.1	[22]
$Ni_{55.2}Mn_{18.6}Ga_{26.2}$	375	unknown	20.4	[23]
$LaFe_{11.6}Si_{1.4}$	200	unknown	14.0	[24]

Figure Captions

Figure 1. The X-Ray diffraction patterns of calculated, observed and differences calculated and observed of annealed $CoMn_{1-x}Ti_xGe$ (x=0.05 (a) and 0.10 (b)) alloys. The green vertical bars indicate the Bragg positions of Hexagonal phase.

Figure 2. The DSC curves of the as-cast and annealed $CoMn_{1-x}Ti_xGe$ (x=0.05 (a) and 0.10 (b)) alloys for heating and cooling mode.

Figure 3. The temperature dependence of magnetization-M(T) curves measured in magnetic field of 150 Oe for as-cast and annealed $CoMn_{1-x}Ti_xGe$ (x=0.05 (a) and 0.10 (b)) alloys.

Figure 4. The magnetic field dependent of magnetization-M(H) curves of as-cast (a) and annealed (b) $CoMn_{0.95}Ti_{0.05}Ge$ alloy.The arrows show the magnetization and demagnetization directions.

Figure 5. The temperature dependence of the entropy change values of as-cast (a) and annealed (b) $CoMn_{0.95}Ti_{0.05}Ge$ alloys.

Figure 6. The phase diagram of the $CoMn_{1-x}Ti_xGe$ alloys. The Curie and structural phase transition temperatures were taken from earlier results for $CoMn_{0.94}Ti_{0.06}Ge$ alloy [21]. PM: paramagnetic, FM: ferromagnetic, Ort.: orthorhombic, Hex: hexagonal. The region shown with red dots represents the unstudied region.

Figure 1

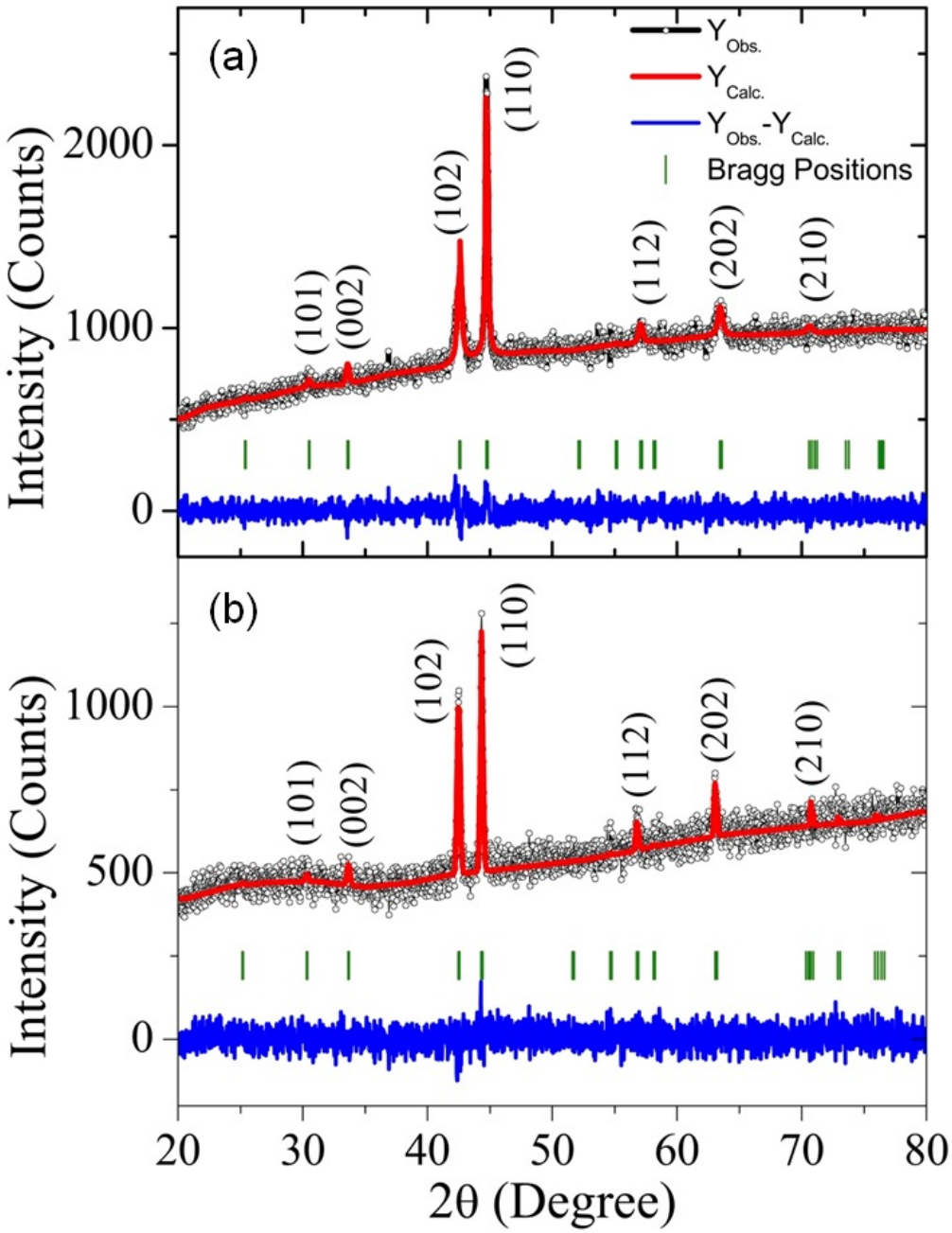
(a)
(b)
$Y_{Obs.}$
$Y_{Calc.}$
$Y_{Obs.}$-$Y_{Calc.}$
Bragg Positions
(101)
(002)
(102)
(110)
(112)
(202)
(210)
Intensity (Counts)
2θ (Degree)
0
1000
2000
500
20
30
40
50
60
70
80

Figure 2

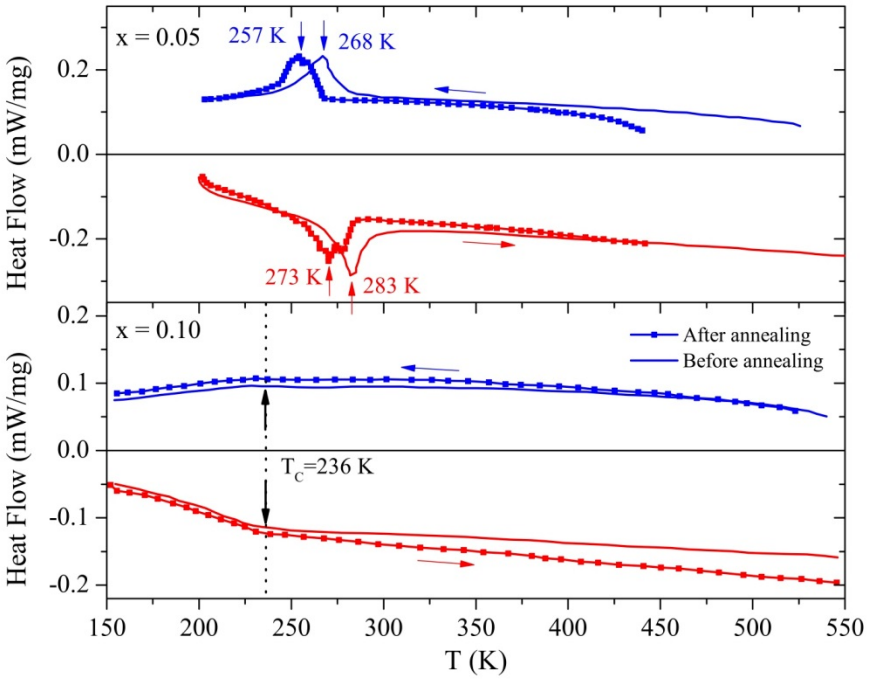
x = 0.05
257 K
268 K
273 K
283 K
x = 0.10
After annealing
Before annealing
T_C=236 K
Heat Flow (mW/mg)
Heat Flow (mW/mg)
T (K)

Figure 3

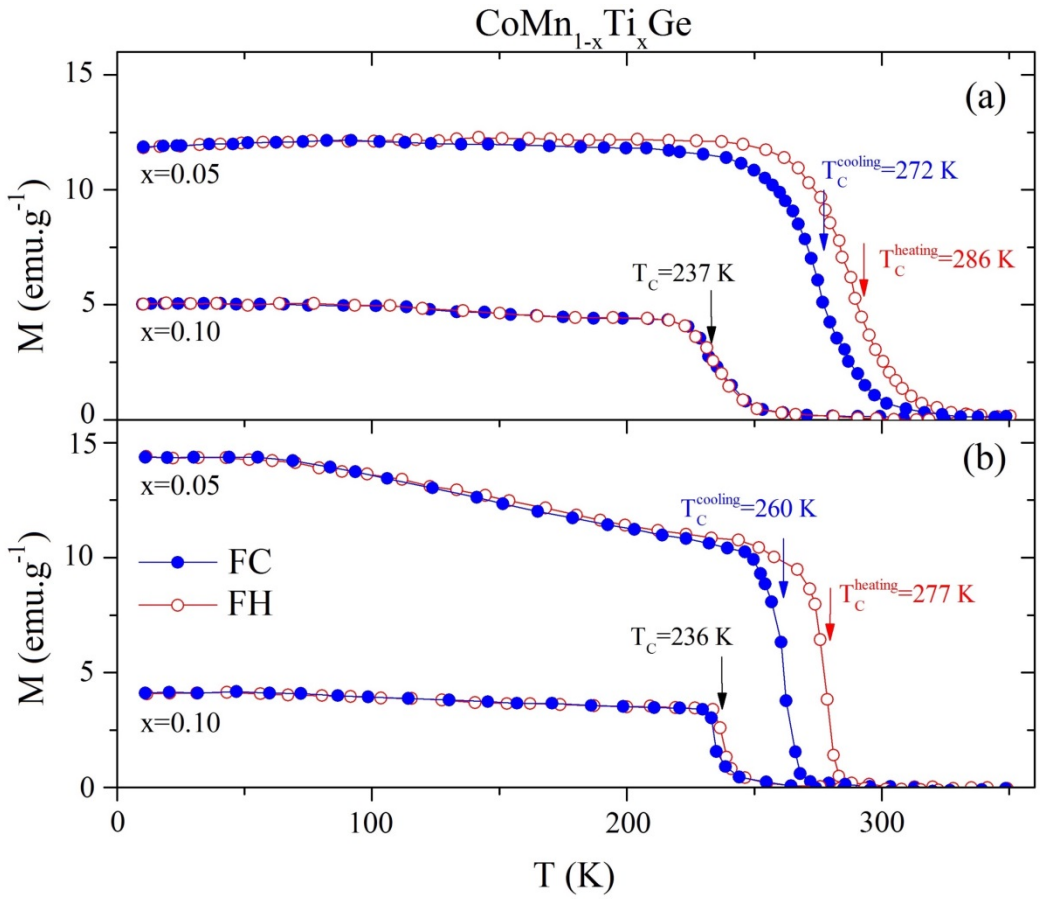
CoMn1-xTixGe
(a)
x=0.05
x=0.10
TCcooling=272 K
TCheating=286 K
TC=237 K
(b)
x=0.05
x=0.10
TCcooling=260 K
TCheating=277 K
TC=236 K
FC
FH
M (emu.g-1)
T (K)
0
5
10
15
0
100
200
300

Figure 4

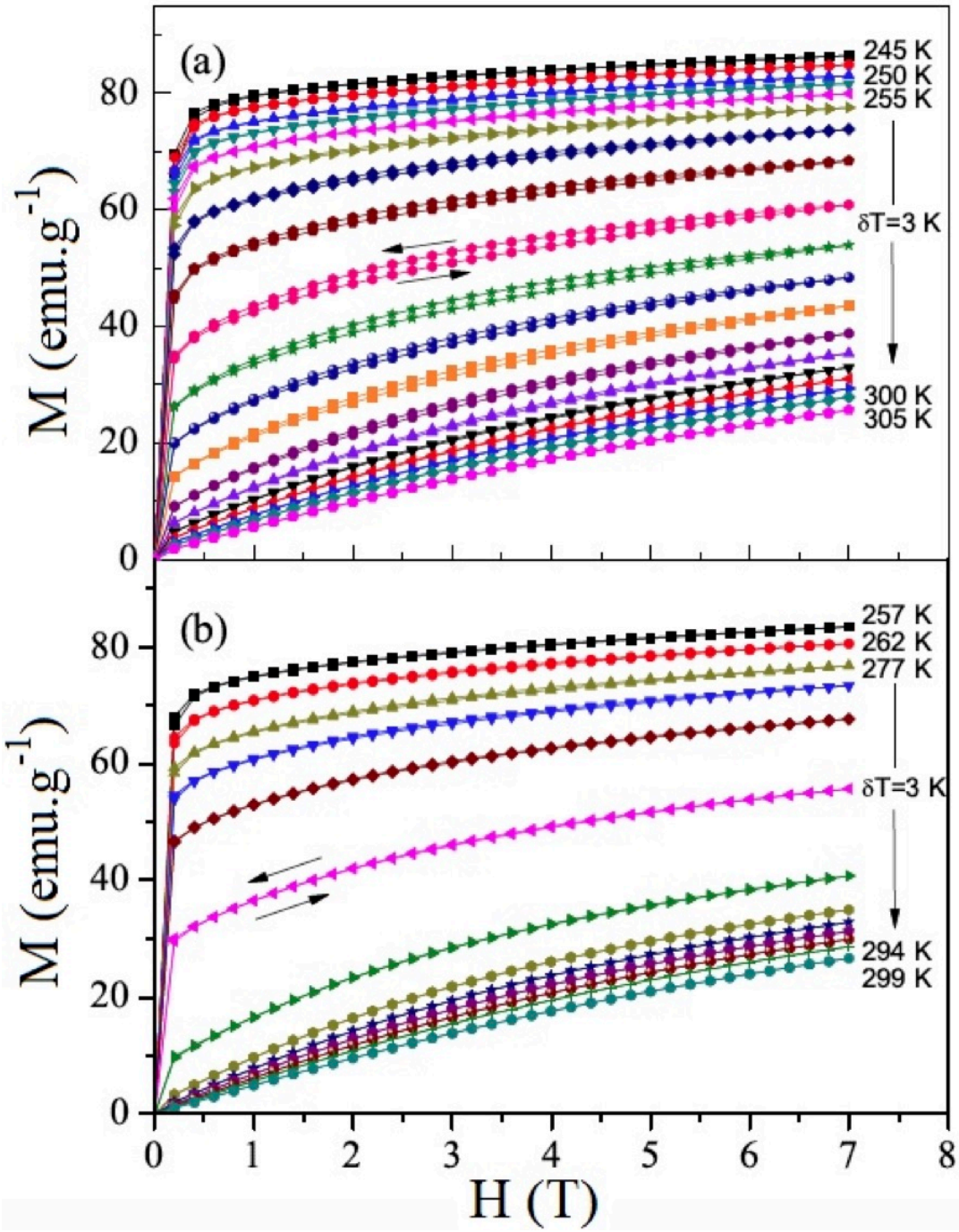
(a)
245 K
250 K
255 K
δT=3 K
300 K
305 K
M (emu.g-1)
(b)
257 K
262 K
277 K
δT=3 K
294 K
299 K
M (emu.g-1)
H (T)

Figure 5

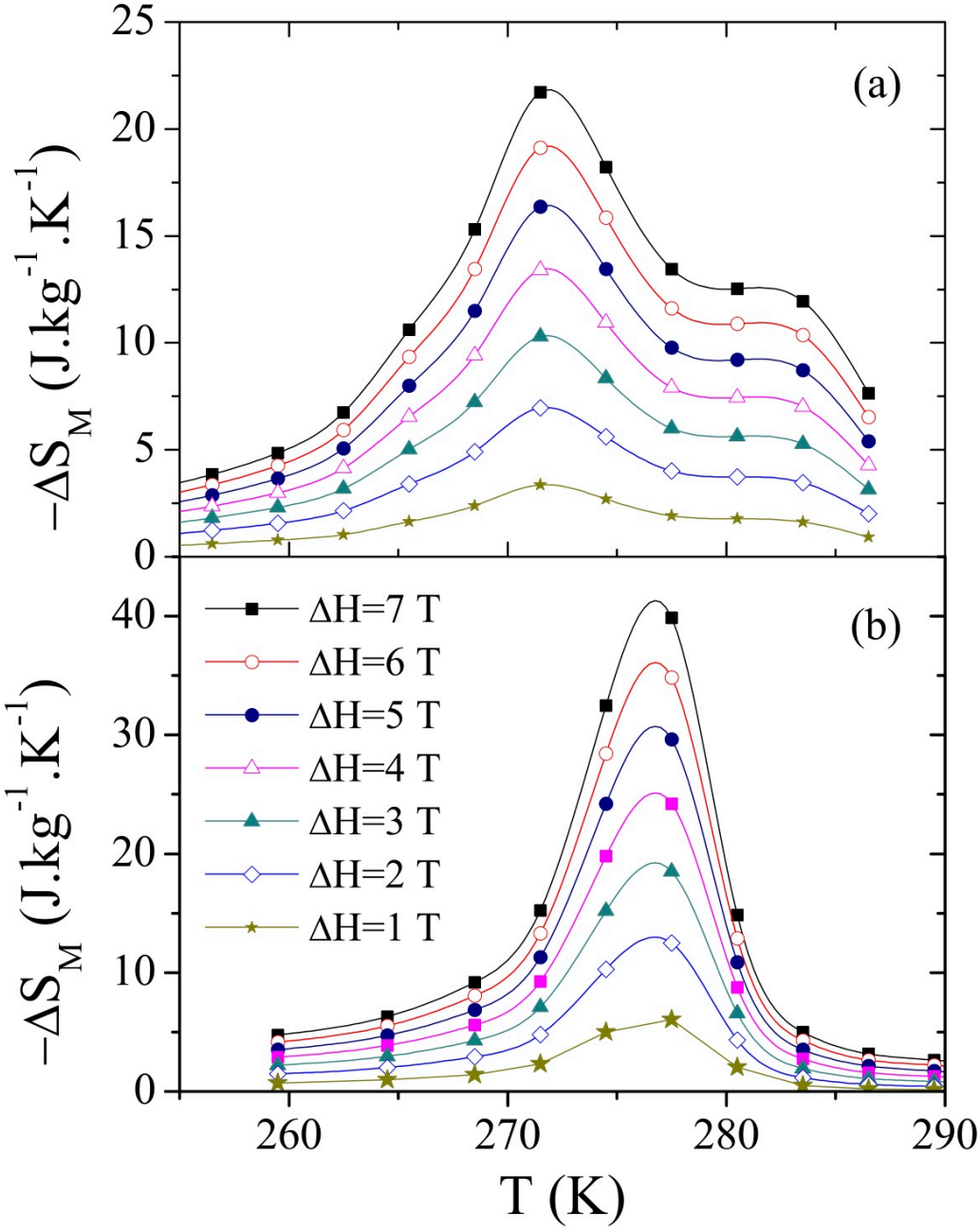
(a)
(b)
ΔH=7 T
ΔH=6 T
ΔH=5 T
ΔH=4 T
ΔH=3 T
ΔH=2 T
ΔH=1 T
−ΔS_M (J.kg^-1.K^-1)
T (K)
0
5
10
15
20
25
30
40
260
270
280
290

Figure 6

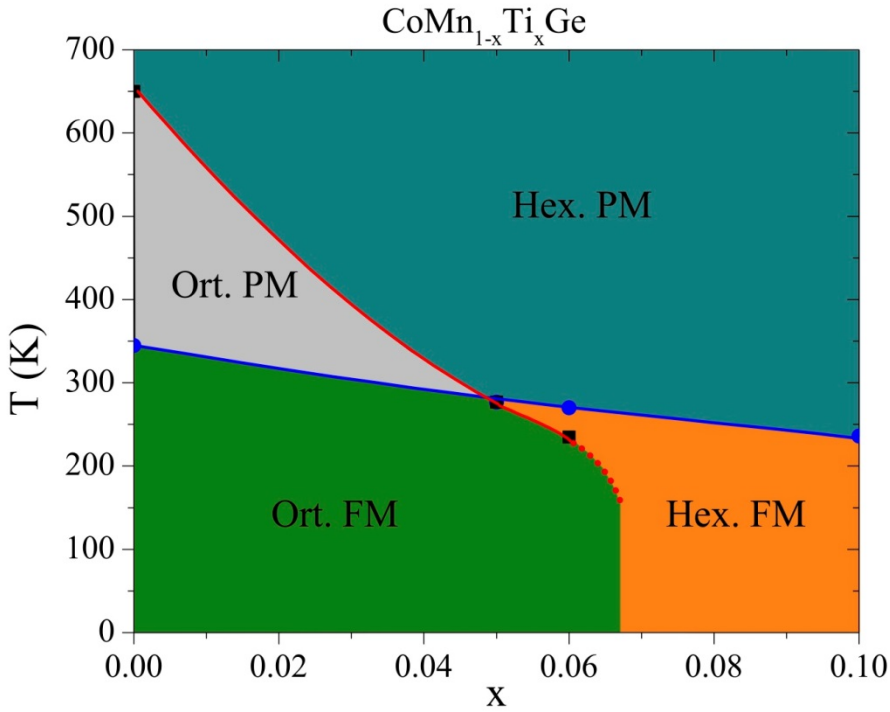
CoMn1-xTixGe
700
600
500
400
300
200
100
0
T (K)
0.00
0.02
0.04
0.06
0.08
0.10
x
Hex. PM
Ort. PM
Ort. FM
Hex. FM